

High-energy neutrino emission from Gamma-Ray Bursts

F. De Paolis, G. Ingrosso, D. Orlando and L. Perrone^{*}

*Dipartimento di Fisica, Università di Lecce and INFN, Sezione di Lecce, Via
Arnesano, CP 193, I-73100 Lecce, Italy*

Abstract

Gamma-Ray Bursts (GRBs) are expected to efficiently accelerate protons up to relativistic energies. High-energy photons can originate from decay of neutral pions produced by the interaction of these protons with the medium surrounding the source. In the same hadronic chain, high energy neutrinos are expected to be produced from decay of charged pions, as well as from decay of generated muons. Neutrinos can travel cosmological distances being much less absorbed than photons, thus providing a powerful tool for the investigation of cosmic sources. In the frame of a recently proposed hadronic model for the emission of high-energy γ -rays, we estimate the neutrino emission from GRBs and calculate the neutrino fluxes at Earth as a function of the model parameters. The detectability of the expected signal by current and future experiments is also extensively discussed.

Key words: Gamma-Ray Burst, Neutrino

PACS: 98.70.R, 95.85.R, 13.15, 25.30.M

1 Introduction

Nowadays, it is widely recognized that GRBs have cosmological origin, as suggested by Beppo-SAX observations [1] of counterparts in the X-ray band of some GRBs. Thanks to these observations, it has been also possible to determine with great accuracy the GRB position and consequently, through pointing of optical and radio telescopes, to evaluate the distance of some GRBs. The derived amount of energy radiated by assuming an isotropic explosion can result in some cases of the order of $\mathcal{E}_\gamma^{iso} \sim 10^{53} - 10^{54}$ erg in the soft γ -ray

^{*} *Corresponding author* - tel +390832-320459 - fax +390832-320505
Email address: lorenzo.perrone@le.infn.it (L. Perrone).

(50 - 300 keV) energy band, showing that in a GRB event up to one solar mass can be radiated in form of soft γ -rays. Note that if GRBs are beamed sources as indicated by afterglow observations [2], the emitted energy would be decreased by the factor $\Delta\Omega/4\pi$, where $\Delta\Omega$ is the beaming angle.

According to the fireball model for GRBs [3], relativistic electrons are accelerated at shock fronts occurring near the interface of the expanding relativistic shells (external shock models), or at shocks forming within the unsteady outflow itself (internal shock models). Soft γ -rays are then produced through leptonic processes, such as synchrotron or Inverse Compton emission.

Many GRBs have been recognized as high-energy γ -rays emitters by the EGRET experiment which detected γ -rays in the energy band between 30 MeV and 20 GeV from a high percentage of the bright bursts found by BATSE [4–6]. These observations clearly show that the GRB phenomenon is not exclusively the domain of soft-energy leptonic processes but may include high-energy hadronic mechanisms.

It has been suggested (see e.g. [7]) that highly relativistic protons accelerated at shock front can produce quite efficiently very high-energy photons and neutrinos through $p\gamma$ interactions within the dense photon field arising from the GRB [8], or by mutual pp interactions in the ejecta [9], or by pn inelastic collisions with neutrons, if present in the original explosion [10].

The emission of high-energy neutrinos and γ -rays has been also investigated within the so-called cannonball scenario, by which jets of highly relativistic balls emitted in supernovae explosions collide with the surrounding shell producing quasi thermal radiation (due to the collision heating), and high energy γ -rays and neutrinos (through pp interaction in the shell) [11]

Very recently, a model for the production of high-energy γ -rays in GRBs with $E_\gamma > 1$ GeV has been proposed [12]: high-energy protons emerging from the GRB source may subsequently interact with external nucleons, giving rise to neutral pions, which in turn promptly decay into high-energy photons. A key requirement of the model is the existence of a dense enough cloud (as a target for pN interactions), which surrounds the GRB source, or, alternatively, situated along the line of sight to the observer and near enough the source. A delay in the arrival times of the high-energy γ -rays with respect to the soft γ -rays and a temporal spread of the signal at Earth is predicted as a consequence of the proton deflection due to the presence of magnetic fields in the region surrounding the GRB source. Clearly, in addition to neutral pion production, inelastic pN collisions also produce charged pions, kaons and small quantities of other mesons. If their main free path for interaction $\lambda_i = (n_N \sigma_{\pi N})^{-1}$, is much larger than their decay path $\lambda_d = \Gamma \tau c$ (with $\Gamma = E_\pi/m_\pi c^2$), they decay into charged leptons and neutrinos [14] ¹. Here n_N is

¹ Note that even in the case of a cloud with density as high as $n_N \simeq 10^{11} \text{ cm}^{-3}$, the

the nucleon number density, $\sigma_{\pi N}$ is the pion-nucleon cross section and τ is the pion proper mean life. The description of this model is given with some detail in section 2. In section 3, we estimate the neutrino emission from GRBs as expected within this frame and compare our results with the theoretical predictions by other models for the production of neutrinos from astrophysical sources. In section 4 we finally discuss the detectability of the expected signal in terms of upward-going neutrino-induced muons by taking into account the experimental constraints given by underground and underwater/ice detectors.

2 The Model

According to [12], we assume that the GRB source emits an amount of energy $\mathcal{E}_p \simeq 10^{54} \Delta\Omega$ erg in form of relativistic protons [13], released at a distance $r_0 \simeq 10^{16}$ cm from the central source, during a time $\Delta t \simeq 1$ s.

Moreover, we require that there exists a dense enough cloud near/around the GRB source (with $n_N \sim 10^9 - 10^{11} \text{ cm}^{-3}$) so that accelerated protons subsequently interact with the nucleons in the cloud ($\sigma_{pN} \sim 3 \times 10^{-26} \text{ cm}^2$), giving rise to neutral and charged pions and ultimately to high-energy photons and neutrinos².

The initial proton flux $J_p(E_p, r)$ is taken to be a function of both the proton energy E_p and the radial coordinate r as in the following:

$$J_p(E_p, r) = C (E_p/\text{GeV})^{-a_p} f(r) \quad [\text{protons cm}^{-2} \text{ s}^{-1} \text{ sr}^{-1} \text{ GeV}^{-1}] . \quad (1)$$

Here, the radial profile, for $r \geq r_0$, has the form

$$f(r) = \begin{cases} \left(\frac{r_0}{r}\right)^2 \exp[-\sigma_{pN} n_N l(E_p, r)] & \text{if } l < R_L(E_p) \\ 0 & \text{if } l > R_L(E_p) , \end{cases}$$

where $R_L(E_p) = E_p/(eB)$ is the proton Larmor radius, $l(E_p, r) \equiv \alpha(E_p, r) R_L(E_p)$ is the path-length travelled by protons starting at r_0 up to their first pN interaction occurring at distance r from the source and $\alpha(E_p, r)$ is the proton

condition $\lambda_d/\lambda_i \ll 1$ is well verified, so that all the produced secondary unstable mesons decay before interacting with the cloud itself.

² The average length travelled by protons in the surrounding medium results to be $\Delta R = (\sigma_{pN} n_N)^{-1} \simeq 10^{-3} \text{ pc } (10^{10} \text{ cm}^{-3}/n_N)$. Correspondingly, the mass enclosed will be $M_{\text{cl}} \sim 0.4 M_\odot (r_0/10^{15} \text{ cm})^2$ in a shell-like cloud geometry around the GRB and $M_{\text{cl}} \sim 0.2 M_\odot (10^{10} \text{ cm}^{-3}/n_N)^2$ in the case of an intervening cloud near the GRB source.

deflection angle due to the intervening magnetic field B (typically $B \simeq 1\mu\text{G}$) given by:

$$\alpha(E_p, r) \simeq \arcsin\left(\frac{r - r_0}{R_L(E_p)}\right), \quad (2)$$

As far as the value of the energy spectral index a_p is concerned, since protons are accelerated by shock waves moving with ultra-relativistic velocities (corresponding to GRB Lorentz factor $\Gamma \simeq 300$, see e. g. [15] and diffusive processes are negligible during the time before pN interactions, we adopt the relevant value $a_p \simeq 2.2$ [16,17].

Finally, the constant C in eq. (1), results from the normalization condition

$$\Delta\Omega \, r_0^2 \int_{E_0}^{+\infty} J_p(E_p, r_0) \, E_p \, dE_p = \frac{\mathcal{E}_p}{\Delta t}, \quad (3)$$

where $E_0 = \Gamma m_p c^2$ is the minimum proton energy.

Following Dermer [18], the production spectrum of high-energy γ -rays resulting from pN collisions, via $\pi^0 \rightarrow \gamma\gamma$ decay, is given by the source function

$$q_\gamma(E_\gamma, r) = 16\pi^2 n_N \int_{E_\pi^{min}}^{+\infty} dE_\pi \int_{E_0}^{+\infty} dE_p \, J_p(E_p, r) \times \int_{\cos\theta_{max}}^1 d\cos\theta \, E^* \frac{d^3\sigma^*}{dp^{*3}} \quad [\gamma \, \text{cm}^{-3} \, \text{s}^{-1} \, \text{GeV}^{-1}], \quad (4)$$

where θ is the angle between the line of sight and the proton direction, asterisks refer to CM frame and $E^* d^3\sigma^*/dp^{*3}$ is the Lorentz invariant cross-section for π^0 production in high-energy ($E_p \lesssim 10^3 \text{ GeV}$) pN collisions³.

Numerical values of $q_\gamma(E_\gamma, r)$ depend on the main model parameters, namely the GRB energetics \mathcal{E}_p , the nucleon number density n_N and the magnetic field strength B (for more details see [12]).

An important effect of the presence of magnetic fields is a temporal spread of the emitted high-energy γ -ray signal on Earth. To better analyze this point, we can consider the proton injection as instantaneous, since the acceleration time $\Delta t \simeq 1 \text{ s}$ is much smaller than the average proton interaction time $(\sigma_{pN} n_N c)^{-1} \simeq 10^5 \text{ s}$ ($10^{10} \text{ cm}^{-3}/n_N$). Accordingly, denoting by t_0 the instant at which photons arrive on Earth in the case $B = 0$ (no proton deflection),

³ Mori [19] had verified that extrapolation up to $E_p \simeq 10^6 \text{ GeV}$ of the invariant cross-section used by Dermer [18] is in reasonable agreement with Monte Carlo simulations by several pN event generators.

the delay $t_i - t_0$ can be expressed as a function of the radial coordinate r_i at which pN interactions occur and the proton Larmor radius $R_L(E_p)$:

$$t_i - t_0 = \frac{R_L(E_p)}{c} \left(\arcsin \frac{r_i - r_0}{R_L(E_p)} - \frac{r_i - r_0}{R_L(E_p)} \right). \quad (5)$$

Vice versa, one can say that photons which arrive on Earth within the time window (t_0, t_i) are produced by protons of energy E_p only if these protons have interacted with nucleons in the shell between r_0 and $r_i(E_p)$.

Correspondingly, the source spectrum $Q_\gamma(E_\gamma; t_0, t_i)$ of γ -rays produced in a GRB event within the temporal window $t_i - t_0$ is given by

$$Q_\gamma(E_\gamma; t_0, t_i) = 16\pi^2 n_N \Delta t \int_{E_\pi^{min}}^{+\infty} dE_\pi \int_{E_0}^{+\infty} dE_p \times$$

$$\int_{r_0}^{r_i(E_p)} dr J_p(E_p, r) \exp[-\sigma_{pN} n_N l(E_p, r)] \times \quad (6)$$

$$\int_{\cos\theta_{max}}^1 d\cos\theta E^* \frac{d^3\sigma^*}{dp^{*3}} \quad [\gamma \text{ GeV}^{-1}] ,$$

with the proton injection time $\Delta t \simeq 1$ s.

In Fig. 1, assuming different values for the model parameters n_N and B in the range $10^9 - 10^{11} \text{ cm}^{-3}$ and $10^{-6} - 10^{-4} \text{ G}$, respectively, we show $Q_\gamma(E_\gamma; 0, 200 \text{ s})$ in the first 200 s, starting from the inset of the signal $t_0 = 0$. From Fig. 1, one can see that for a given photon energy E_γ the differential γ -ray production increases with increasing n_N and decreasing B . The effect is particularly important at low E_γ values. In fact, low-energy photons are mainly generated by low-energy protons with E_p roughly one order of magnitude above E_γ : they are more easily deflected by the intervening magnetic fields giving rise to photons that cannot reach the observer since $\alpha(E_p, r) > \pi/2$. However, our numerical results show that in a large range of values for n_N and B , the decrease of $Q_\gamma(E_\gamma; t_0, t_i)$ for increasing values of B can be counterbalanced by increasing n_N . Moreover, for each assumed value of B , there exists a limiting density ($n_N \simeq 10^{11} \text{ cm}^{-3}$ in the case $B \simeq 1 \mu\text{G}$) above which most of the protons interact before suffer substantial deflection.

Note that in deriving eq. (6) we have neglected re-absorption of the produced γ -rays in the cloud itself⁴. Clearly, re-absorption of neutrinos within the

⁴ High-energy γ -rays may in principle be re-absorbed through the interactions with the atomic hydrogen, provided that the path they have to travel inside the cloud (after being produced) is long enough. However, clouds nearby the GRB source are expected to present a high ionization degree, so that the relevant absorption

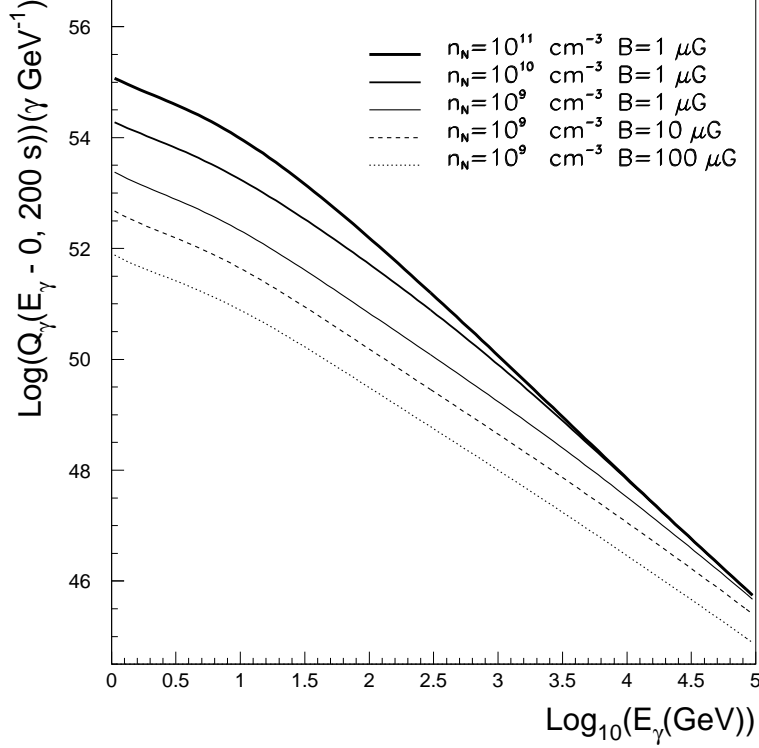


Fig. 1. The source γ -ray spectrum $Q_\gamma(E_\gamma; 0, 200 \text{ s})$ in the first 200 s of the signal life for different values of the cloud number density $n_N = 10^9 - 10^{11} \text{ cm}^{-3}$ and of the magnetic field strength $B = 10^{-6} - 10^{-4} \text{ G}$. The GRB total energetics is assumed to be 10^{54} erg/sr .

cloud itself can be completely neglected.

3 High-energy neutrino emission

It is well known that, for a proton power law spectrum $J_p(E_p) \propto E_p^{-a_p}$ and inclusive cross sections for meson production obeying Feynman scaling, the produced spectrum of γ -rays, ν_e 's, ν_μ 's and ν_τ 's are all proportional at high energies (see e. g. [20]) Following the calculation developed by Dar [21] and by Lipari [22], we assume in particular that muon neutrino and gamma ray spectra by pN interactions are related through $Q_{\nu_\mu} \sim KQ_\gamma$ with $K \sim 0.7$. From eq. (6), we can then estimate the differential neutrino fluences on Earth

processes are γe and γp interactions, which imply a large γ free-path before re-absorption.

within the time interval $t_i - t_0$

$$F_\nu(E_\nu; t_0, t_i) = \frac{Q_\nu[E_\nu(1+z); t_0, t_i] (1+z)}{4\pi D_L^2(z)} \quad [\nu \text{ cm}^{-2} \text{ GeV}^{-1}] , \quad (7)$$

where z is the GRB redshift and

$$D_L(z) = \frac{c}{H_0 q_0^2} \left(z q_0 + (q_0 - 1)(-1 + \sqrt{2q_0 z + 1}) \right) \quad (8)$$

is the GRB luminosity distance, with $H_0 \simeq 70 \text{ km s}^{-1} \text{ Mpc}^{-1}$ and $q_0 \simeq 0.15$. In Fig. 2, assuming $z = 1$ and $\mathcal{E}_p = 10^{54} \text{ erg/sr}$, the neutrino fluence $F_\nu(E_\nu; 0, 200 \text{ s})$ in the initial 200 s is given as a function of neutrino energy for selected values of n_N and B parameters. A comparison with Fig. 1 shows that, apart the energy z shift, the neutrino fluence follows, as a function of model parameters, the same behaviour of the source γ -ray spectrum.

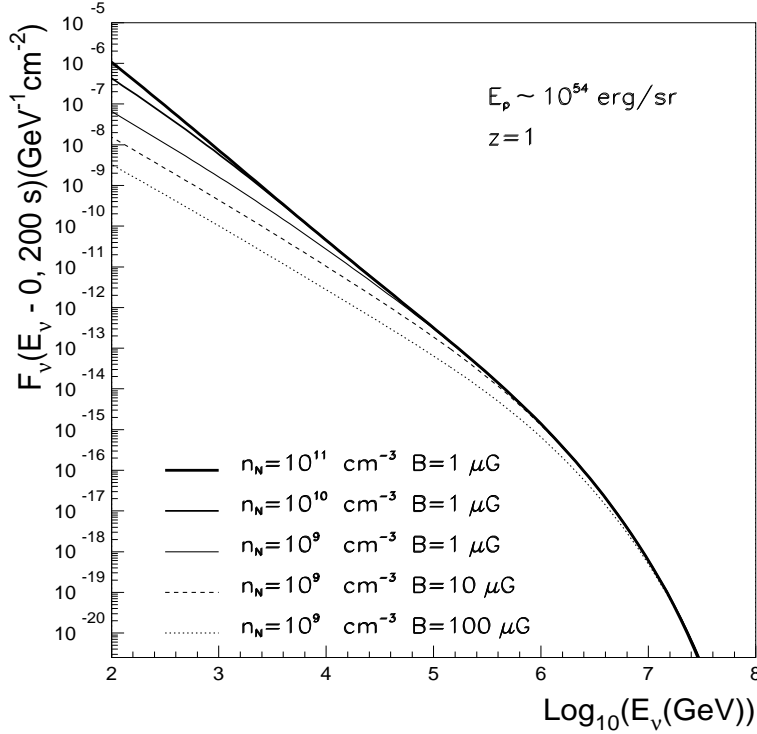


Fig. 2. Expected $\nu_\mu + \bar{\nu}_\mu$ neutrino fluences $F_\nu(E_\nu; 0, 200 \text{ s})$ in the first 200 s of the signal life for different values of the cloud number density $n_N = 10^9 - 10^{11} \text{ cm}^{-3}$ and of the magnetic field strength $B = 10^{-6} - 10^{-4} \text{ G}$. The GRB total energetics and redshift are assumed to be 10^{54} erg/sr and $z = 1$, respectively.

Starting from the neutrino fluence $F_\nu(E_\nu; t_0, t_i)$ during the time interval $t_i - t_0$, one can estimate an average neutrino flux on Earth from a single source as

follows:

$$\langle \Phi_\nu(E_\nu) \rangle = \frac{F_\nu(E_\nu; t_0, t_i)}{t_i - t_0}. \quad (9)$$

Otherwise, it is also possible that neutrinos from unresolved GRBs sources give a contribution to the diffuse high energy neutrino background. In this respect, due to the widely accepted cosmological origin of GRBs, we adopted, as recently done in [23], the cosmological evolution scheme developed by Schmidt [24]. In particular, we assume that the rate of GRB events, per unit comoving volume and per unit comoving time, is given by

$$\dot{n}(z) = \begin{cases} \dot{n}_0(1+z)^p & \text{for } 0 < z < z_p \\ \dot{n}_0(1+z_p)^p & \text{for } z > z_p \end{cases}$$

with $z_p = 1$ and $p = 3.32$. The parameter \dot{n}_0 is then determined so that the observed (in the soft γ -ray band) total GRB event rate

$$\dot{N}_{GRB} = \int_0^{z_{max}} \frac{\dot{n}(z)}{1+z} \frac{dV}{dz} dz \quad (10)$$

reads $\dot{N}_{GRB} \simeq 10^3 \text{ yr}^{-1}$. Here, $dV = 4\pi D_M^2 dD_M$ is the comoving volume element, $D_M = D_L/(1+z)$ is the proper motion distance, related to the luminosity distance D_L given in eq. (8), z_{max} is taken equal 5. Moreover, in eq. (10) we also take into account that the time interval between bursts is stretched by the factor $(1+z)$.

For simplicity, we assume that GRBs are standard candles, each source with $\mathcal{E}_p = 10^{54} \text{ erg/sr}$, $B = 1\mu\text{G}$ and $n_N = 10^9 \text{ cm}^{-3}$. Correspondingly, the diffuse neutrino flux expected on Earth results to be

$$\Phi_\nu(E_\nu) = \int_0^{z_{max}} \frac{Q_\nu[E_\nu(1+z); 0, +\infty]}{4\pi D_L^2(z)} \frac{\dot{n}(z)}{1+z} \frac{dV}{dz} dz \quad (11)$$

In Fig. 3, $\Phi_\nu(E_\nu)$ is given as a function of E_ν . For comparison we show the diffuse neutrino flux from GRB events (via $p\gamma$ interactions) predicted by the Waxman & Bahcall model [8] as well as the upper bound implied by high energy cosmic ray observations estimated by the same authors [25]. Moreover, in Fig. 3, we give the atmospheric neutrino flux averaged on the zenith angle as calculated by Gaisser et al. [26]. Actually, at energy above 10 TeV, the isotropic contribution of neutrinos produced in the atmosphere by the semileptonic decays of charmed hadrons (prompt neutrinos), starts to dominate over the conventional pion and kaon decay induced atmospheric neutrino flux. In Fig. 3 we report the contribution of prompt neutrinos as calculated in [27] within the frame of the Recombination Quark Parton Model. It should be remarked that

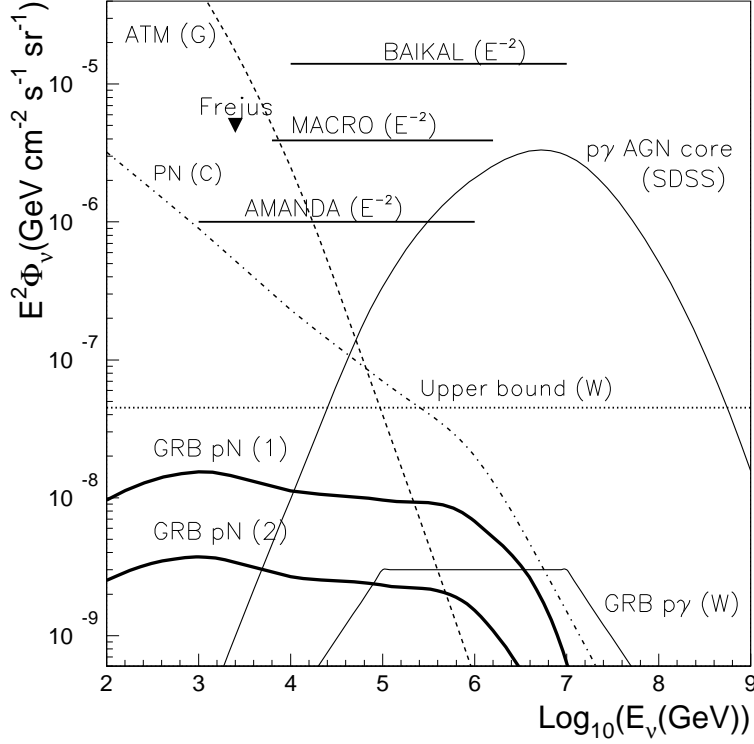


Fig. 3. Diffuse fluxes of $\nu_\mu + \bar{\nu}_\mu$ from this model assuming no evolution [GRB pN (1)] and Schmidt's evolution [GRB pN (2)], respectively. The predictions according to other models of AGNs and GRBs are also shown: SDSS [31], W [25]. The dashed curve refers to the angle average atmospheric neutrino flux [26]; the dash-dotted line refers to the flux of prompt neutrinos according to one of the highest predictions given in [27]; the dotted line is the theoretical upper bound to neutrino flux from astrophysical sources as calculated in [25]. Some current experimental upper limits are also shown: AMANDA [32], MACRO [33], Frejus [28] and BAIKAL [30].

there is some theoretical uncertainty on the calculation of prompt neutrinos flux, as well as on the energy at which this contribution crosses over the conventional atmospheric flux. In Fig. 3, we considered one of the highest prediction among those given in [27]. Finally, the upper limits from current experiments (Frejus [28], AMANDA [29] and BAIKAL [30]) are shown, derived by assuming a power law spectrum ($\propto E_\nu^{-2}$) an initial neutrino flux.

4 Neutrino signal detectability

4.1 Neutrino propagation

High-energy neutrinos from astrophysical sources can be detected by collecting the upward-going neutrino-induced muons produced through charge-current interactions with the matter surrounding the detector. Based upon this detection principle, current underground and underwater/ice experiments are surveying the sky in order to search for neutrino sources. In the frame of the model described above, we have investigated by numerical calculation the detectability of the signal expected either from a single point-like GRB, or from the diffuse flux due to unresolved GRBs. Neutrino propagation through the Earth has been developed following the approach discussed in [34], where they give an analytical method for the precise calculation of the spectrum of high energy neutrinos propagating through a dense medium of any thickness, for initial spectrum and for cross sections of any form.

As a preliminary observation, it should be noticed that the results of atmospheric neutrino experiments [35,36] suggest that muon neutrinos can oscillate into tau neutrinos, thus affecting the expected muon event rate on the detector. This effect has been extensively discussed e.g. in [37]. Here, flavour oscillation will be not considered.

At energy above 1 GeV neutrino-matter interaction is dominated by the process of *deep inelastic scattering* (DIS) on nucleons (charge and neutral current processes), since the contributions of both elastic and quasi-elastic interactions become negligible. The main difficulty for the evaluation of the deep inelastic neutrino-nucleon cross sections arises from the fact that, in spite of the lack of experimental data, at very high energy the details of nucleon structure become important.

Detectable muons are produced through charge current interaction as in eq. (12). Neutral current interaction described by eq. (13) causes instead a modulation in the spectrum of the interacting neutrinos.

$$\nu_\mu(\bar{\nu}_\mu) + N \rightarrow \mu^-(\mu^+) + X , \quad (12)$$

$$\nu_\mu(\bar{\nu}_\mu) + N \rightarrow \nu_\mu(\bar{\nu}_\mu) + X' . \quad (13)$$

The total cross section for these processes can be written in terms of differential cross sections as follows:

$$\sigma_{tot}^{cc}(E_\nu) = \int_0^{1-\frac{m_\mu}{E_\nu}} \frac{d\sigma^{cc}}{dy}(E_\nu, y) dy , \quad (14)$$

$$\sigma_{tot}^{nc}(E_\nu) = \int_0^1 \frac{d\sigma^{nc}}{dy}(E_\nu, y) dy , \quad (15)$$

where E_ν is the energy of the incoming neutrino, m_μ is the muon mass and y is defined by E_l/E_ν with $E_l = E_\nu - E_\mu$ for charge current interaction (E_μ

is the energy of the outgoing muon) and $E_l = E_\nu - E'_\nu$ for neutral current interaction (E'_ν is the energy of the outgoing neutrino).

Let $F_\nu(E_\nu, x)$ be the differential energy spectrum of neutrinos at a column depth $x = \int_0^L \rho(L') dL'$, where $\rho(L)$ is the density of the medium at distance L from the boundary, measured along the neutrino beam path. The one-dimensional transport equation can be expressed in the form [34]:

$$\frac{\partial F_\nu(E_\nu, x)}{\partial x} = -\frac{F_\nu(E_\nu, x)}{\lambda_\nu(E_\nu)} + \int_0^1 \frac{N_A}{A_N} \frac{d\sigma^{nc}}{dy} F_\nu\left(\frac{E_\nu}{1-y}, x\right) \frac{dy}{1-y}, \quad (16)$$

with the boundary condition $F_\nu(E_\nu, 0) = F_\nu^0(E_\nu)$. Here, $\lambda_\nu(E_\nu)$ is the neutrino interaction length in g cm^{-2} defined by:

$$\lambda_\nu(E_\nu) = \frac{1}{(N_A/A_N)(\sigma_{tot}^{cc}(E_\nu) + \sigma_{tot}^{nc}(E_\nu))}, \quad (17)$$

where N_A is the Avogadro number and $A_N = 1 \text{ g mol}^{-1}$.

The first term in the right side of eq. (16) accounts for the absorption of neutrinos of energy E_ν , due to charge and neutral current interactions; the second term describes the additive contribution of higher energy neutrinos “regenerating” through neutral current interaction at energy E_ν . The solution of eq. (16) is taken of the form

$$F_\nu(E_\nu, x) = F_\nu^0(E_\nu) \exp\left[-\frac{x}{\Lambda_\nu(E_\nu, x)}\right], \quad (18)$$

where the function $\Lambda_\nu(E_\nu, x)$ is the effective absorption length containing the relevant information on the modulation of the neutrino flux $F_\nu(E_\nu, x)$ along the propagation (see Ref. [34] for further details). The differential $\nu_\mu N$ and $\bar{\nu}_\mu N$ cross sections have been calculated by using the approach in Ref. [38] based on the renormalization-group-improved parton model and on the last available experimental information about the quark structure of the nucleon. They are written in terms of the Bjorken scaling variables y and $\hat{x} = Q^2/2ME_l$, where $-Q^2$ is the invariant momentum transferred between the incoming neutrino and the outgoing lepton (muon or neutrino, for charge and neutral current interaction, respectively). The detailed formulas used for the calculation are given in [38].

Various versions of different sets of parton density functions $q(\hat{x}, Q^2)$ are collected in a large CERN software library PDFLIB [39]; they can be simply accessed by setting few parameters to choose the desired version. In this calculations, we selected the third version of the CTEQ collaboration model [40] for the next-to-leading order (NLO) quark distributions in the deep-inelastic scattering factorization scheme. The CTEQ3 distributions are particularly suitable for high energy calculations since the numerical evolution is provided for very low \hat{x} . Unfortunately, the uncertainty due to this extrapolation may be rather large and is hard to estimate. The Q^2 evolution is realized by the NLO

Gribov-Lipatov-Altarelli-Parisi equations from initial $Q_0^2 = 2.56 \text{ GeV}^2$. (The new version of parton density functions by CTEQ group [41] doesn't produce significant changes for this calculation).

Fig. 4 shows the neutrino interaction length $\lambda_\nu(E_\nu)$ for deep inelastic scattering off an isoscalar nucleon $N = (n + p)/2$ ($n \rightarrow$ neutron, $p \rightarrow$ proton), for ν_μ (solid line) and $\bar{\nu}_\mu$ (dashed line). The dotted line placed at the level of the Earth diameter demonstrates that the Earth becomes opaque to neutrinos with energy exceeding the TeV energy-range.

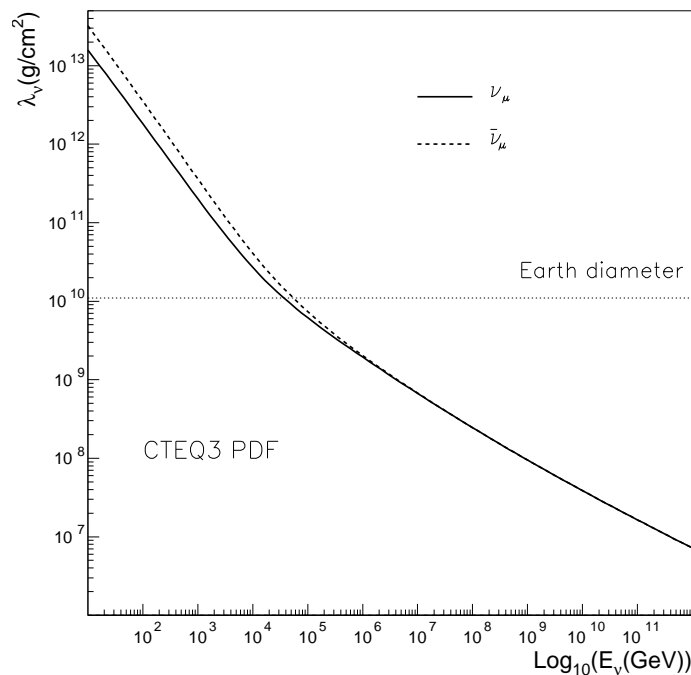


Fig. 4. Neutrino interaction length for deep inelastic scattering off an isoscalar nucleon $N = (n + p)/2$, for ν_μ (solid line) and $\bar{\nu}_\mu$ (dashed line). The calculation has been done for the CTEQ3 set of parton density functions [40]. The dotted line gives the Earth diameter.

4.2 Muon propagation

High energy muons propagating through matter mainly interact by quasi-continuous (ionization) and discrete (e^+e^- pair production, bremsstrahlung and photonuclear interaction) electromagnetic scattering. Ionization dominates at energy lower than few hundreds of GeV , whereas above the TeV region energy losses are mainly due to radiative processes.

At this stage, muon propagation has been treated analytically, according to the approach suggested in [42]. Following [42], the one-dimensional transport

equation can be written as:

$$\frac{\partial F_\mu(E_\mu, x)}{\partial x} = \frac{\partial}{\partial E_\mu}(\beta(E_\mu)F_\mu(E_\mu, x)) + \mathcal{G}(E_\mu, x), \quad (19)$$

with the boundary condition

$$F_\mu(E_\mu, 0) = 0.$$

Here, $F_\mu(E_\mu, x)$ is the muon flux at energy E_μ and depth x , $\beta(E_\mu)$ is the average total energy loss per unit length due to electromagnetic muon scattering (ionization plus radiative processes) and $\mathcal{G}(E_\mu, x)$ is the “source” function introduced to describe the production of muons through neutrino charge current interaction. $\mathcal{G}(E_\mu, x)$ is given by:

$$\mathcal{G}(E_\mu, x) = \frac{N_A}{A_N} \int_0^1 \frac{d\sigma^{cc}}{dy} \left(\frac{E_\mu}{1-y}, y \right) F_\nu \left(\frac{E_\mu}{1-y}, x \right) \frac{dy}{1-y}. \quad (20)$$

The solution of eq. (19) can be written in the form:

$$F_\mu(E_\mu, x) = \int_{E_\mu}^{\mathcal{E}(E_\mu, x)} \frac{dE'_\mu}{\beta(E'_\mu)} \mathcal{G}(E'_\mu, x - \mathcal{R}(E'_\mu, E_\mu)), \quad (21)$$

where the function $\mathcal{R}(E'_\mu, E_\mu)$ defined by

$$\mathcal{R}(E'_\mu, E_\mu) = \int_{E_\mu}^{E'_\mu} \frac{dE''_\mu}{\beta(E''_\mu)} \quad (22)$$

represents the mean depth crossed by a muon of initial energy E'_μ and final energy E_μ ; $\mathcal{E}(E_\mu, x)$ labels the initial energy needed by a muon to reach the depth x with final energy E_μ . The calculation of muon energy losses is crucial to correctly evaluate the expected muon flux on the detector. The muon energy losses due to radiative processes (e.g. e^+e^- pair production, bremsstrahlung and photonuclear interaction) can be expressed in terms of differential cross section for the specific muonic interaction process k as follows:

$$-\left\langle \frac{dE}{dx} \right\rangle_k = \frac{N_A}{A} E_\mu \int_{v_{min}}^{v_{max}} v \frac{d\sigma^k}{dv}(v, E_\mu) dv, \quad (23)$$

where N_A and A are Avogadro’s number and the mass number respectively; v is the fraction of initial energy E_μ lost by muon at the occurrence of the process k ; v_{min} and v_{max} are the kinematical limits for the allowed values of v ; x is the thickness of crossed matter, expressed in g cm^{-2} . The total average muon energy losses $\beta(E_\mu)$ results from the sum of the radiative interaction terms plus the quasi-continuous contribution due to ionization. The explicit formulas used in this work are given in [43], accordingly to the theoretical framework discussed in the standard reference by Lohmann and Voss [44]. Fig. 5 shows

the total average muon energy loss (thick line) and the contributions from the single electromagnetic process.

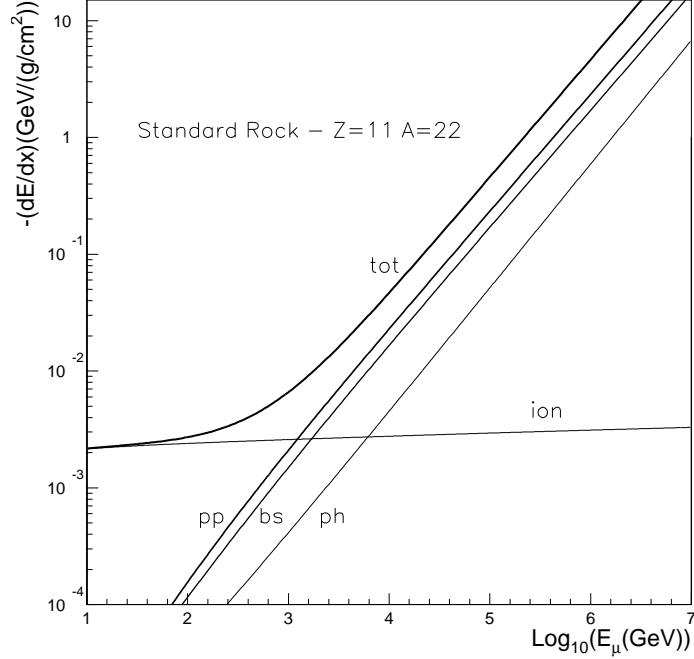


Fig. 5. Total average muon energy losses in standard rock (thick line). The contributions of each electromagnetic process have been also plotted, *ion* \rightarrow ionization, *pp* $\rightarrow e^+e^-$ pair production, *bs* \rightarrow bremsstrahlung, *ph* \rightarrow photonuclear interaction.

4.3 Discussion and results

In Fig. 6, assuming the same parameter values adopted in Fig. 2, we give the expected number of events per cm^2 from a single GRB source, as a function of the cosine of zenith angle θ .

The dependence on θ of the muon flux is a consequence of neutrino absorption in Earth, which cannot be neglected at high energy. Moreover, the suppression at $\cos \theta \leq -0.8$ reflects the hard discontinuity of Earth density profile in correspondence of the massive nucleus. In particular, in Fig. 6 the calculated fluxes are compared with upper limits by experiments (MACRO [45], IMB [46], and AMANDA [29]). (Note that the IMB limit has been lowered for convenience of presentation. Moreover, the AMANDA limit, shown as a dashed line, has been estimated starting from the declared upper limit on neutrino flux). Finally, for comparison purposes, in Fig. 6 we show the number of events calculated by assuming as theoretical input the well-known Waxman

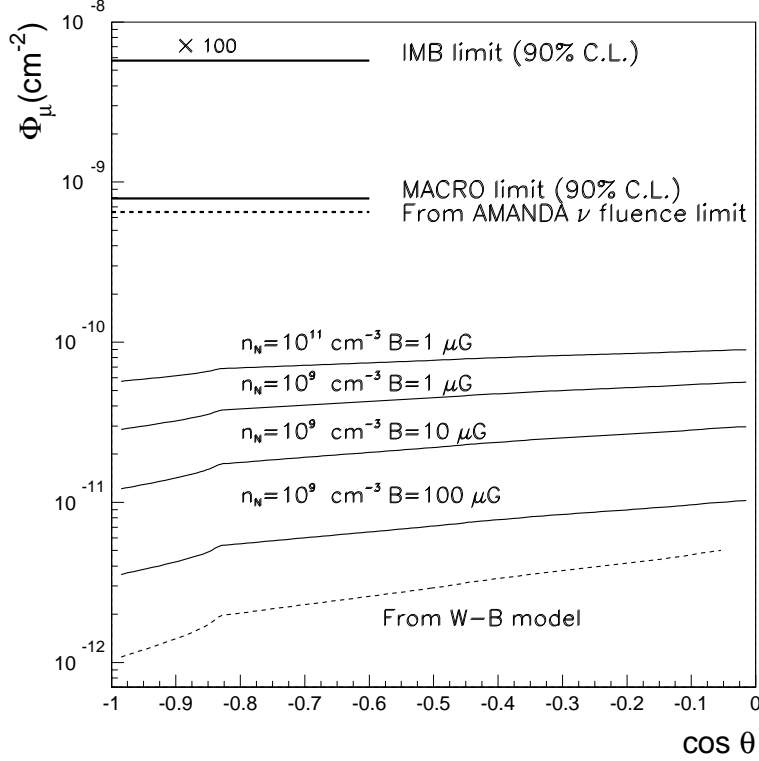


Fig. 6. The total number of events per cm^2 expected from a single GRB as a function of the cosine of zenith angle θ . The plot is shown for the set of model parameters given in Fig. 2. The thin dashed line is calculated starting from the model by Waxman and Bahcall [25]. Upper limits by experiments MACRO [45], IMB [46], and AMANDA [29] are also shown (see text for comments).

and Bahcall ([8]) model of neutrino production from GRBs. The sensitivity to gamma ray bursts as point-like sources is improved by the search for space and time correlation with optical information. In this case the background is strongly suppressed.

The same analytical procedure has been used in order to calculate the expected number of events induced by our predicted neutrino flux from unresolved GRBs labelled in Fig. 3 as GRB pN (1) and (2). The overall rate of events expected for $E_\mu > 10$ GeV is 190 and 46 events per km^2 from the entire lower Earth hemisphere for the flux (1) and (2) respectively. The event rate for $E_\mu > 10$ TeV, in a range where the signal is expected to start arising over the atmospheric neutrino background, becomes 26 and 6 events per km^2 respectively. In any case a good knowledge of the background is required in order to have a reliable measure.

As shown in Fig. 3 and Fig. 6, current experiments have not the required sensitivity to exclude or confirm our predictions. Neutrinos telescopes of the

next generation like ANTARES [47], NEMO [48], NESTOR [49], with effective area ranging from 0.1 to 1 km², will be likely capable to success in this task.

5 Conclusions

We have presented a model for the production of high energy neutrinos from GRBs in an energy range from few GeV up to few PeV, through the interaction of the shock accelerated protons with the matter surrounding the source. The results have been compared with other theoretical predictions and with the available experimental upper limits from underground and underwater/ice neutrino detectors. Current experiments have not the required sensitivity to exclude or confirm our predictions but the next generation neutrinos telescopes are expected to be capable to reach this goal in few years of data taking.

6 Acknowledgment

We wish to acknowledge the members of the MACRO collaboration, in particular the Lecce group, for the fruitful discussion and the concrete help. A further acknowledgment goes to INFN which contributed to support this research. We also thank Prof. P. Galeotti for interesting discussions.

References

- [1] Costa E., Frontera F., Heise J., et al., 1997, Nat 387, 783
- [2] Huang Y. F., Dai Z. G., Lu T., 1999, astro-ph 0002433
- [3] Rees M.J., Mészáros P., 1992, MNRAS 304, L31
- [4] Schneid E.J., Bertsch D.L., Fichtel C.E., et al., 1992, A&A 255, L13
- [5] Schneid E.J., Bertsch D.L., Dingus B.L., et al., 1995, ApJ 453, 95
- [6] Hurley K., Dingus B.L., Mukherjee R., et al., 1994, Nat 372, 652
- [7] Berezhinsky V.S., Castagnoli C., Galeotti P., 1985, Il Nuovo Cimento, 8C-3, 185
- [8] Waxman E., Bahcall J. 1997, Phys. Rev. Lett. 78, 2292
- [9] Paczynski B., Xu G. 1994, ApJ 427, 708
- [10] Bahcall J., Meszaros P. 2000, astro-ph 0004019

- [11] Dar A., De Rùjula A., 2001, astro-ph/0105094
- [12] De Paolis F., Ingrosso G., Orlando D., 2000, A&A 359, 514
- [13] Totani T., 1999, Mont. Not. Royal Astr. Soc., 307, L41
- [14] Berezhinsky V.S., et al., 1990, *Astrophysics of Cosmic Rays*, North Holland
- [15] Piran T., 1999, Phys. Rep. 314, 575
- [16] Bednarz J., Ostrowski M., 1998, Phys. Rev. Lett. 80, 3911
- [17] Vietri M., 2000, astro-ph/0002269
- [18] Dermer C.D., 1986, A&A 157, 223
- [19] Mori M. 1997, ApJ. 478, 225
- [20] Gaisser T., *Cosmic Rays and Particle Physics* 1990, Cambridge University Press
- [21] Dar A. 1983, Phys. Rev. Lett. 51, 227
- [22] Lipari P. 1993, Astroparticle Phys. 1, 195
- [23] Stecker F. W., 2000, Astrop. Phys. 14, 207
- [24] Schmidt M., 1999, ApJ 523, L117
- [25] Waxman E., Bahcall J., 1998, Phys Rev. D 59, 023002
- [26] Gaisser T., Halzen F., Stanev T., 1995, Phys. Rep. 258, 173
- [27] Costa, C. G. S., hep-ph/0010306
- [28] Rhode W., Frejus Coll., 1996, Astropart. Phys., 4, 217
- [29] Carlton Bay C., Ph.D. Thesis, astro-ph/0008255
- [30] Balkanov V.A., BAIKAL Coll. 2000, Astroparticle Phys. 14, 61
- [31] Stecker F. W., Done C., Salamon M. H. and Sommers P., 1991, Phys. Rev. Lett., 66, 2697; Erratum-ibid., 1992, 69, 2738
- [32] Halzen, F., 2000, talk given to Now 2000
- [33] Perrone L., MACRO Collaboration, to appear on Proc. of the NATO - Advanced Research Workshop on “Cosmic Radiations: from Astronomy to Particle Physics” 2001, Ojuda - Morocco; to appear on Proc. of 27th ICRC, 2001, Hamburg - Germany
- [34] Naumov V. A., Perrone L., 1999, Astrop. Phys. 10, 239
- [35] Fukuda Y., Super-Kamiokande Collaboration, Phys. Rev. Lett., 1999, 82, 2644
- [36] Ambrosio M., MACRO Collaboration, 1998, Phys. Lett. B 434, 451
- [37] Dutta S.I., Reno M.H., I. Sarcevic, 2000, Phys. Rev. D 62, 123001

- [38] Gandhi R., Quigg C., Reno M. Sarcevic I., 1998, Phys. Rev. D, 58, 093009
- [39] Plathow-Besch H., 1997, “PDFLIB, Version 7.09”, CERN-PPE report 1997.07.02; Plathow-Besch H., 1993, Comp. Phys. Comm., 75, 396
- [40] Lai H. L. et al., 1995 (CTEQ Coll.), Phys. Rev. D 51, 4763
- [41] Lai H.L., CTEQ Collaboration, 2000, Eur. Phys. J. C, 12, 375
- [42] Naumov V.A., Sinegovsky S.I., Bugaev E.V., Yad. Fiz. **57**, 439 (1994) [Phys. Atom. Nucl. **57**, 412 (1994)]; Proc. of the 2nd NESTOR International Workshop, Fortress of Niokastro, Pylos, Greece, October 19-22, 1992, ed. by L. K. Resvanis, 119 (see also hep-ph/9301263)
- [43] Bottai S., Perrone L., 2001, Nucl. Instr. and Meth. A, 459, 319
- [44] Lohmann W., Kopp R., Voss R., 1985, CERN yellow report 85-03
- [45] Ambrosio M., MACRO Coll., 2001, Ap. J., 546, 1038
- [46] Szendy B. et al., 1995, ApJ 444, 415
- [47] Carloganu C., ANTARES Coll., 2000, Nucl. Phys. Proc. Suppl., 85, 146
- [48] De Marzo C., NEMO Coll., 2000, Nucl. Phys. Proc. Suppl., 87, 433
- [49] Resvanis L. K., NESTOR Coll. 2000, Nucl. Phys. Proc. Suppl., 87, 448